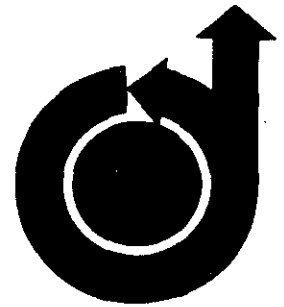# No. 68-83

AERODYNAMICS SHATTERING OF LIQUID DROPS

by

A. A. RANGER and J. A. NICHOLLS
University of Michigan
Ann Arbor, Michigan

AIAA Paper
No. 68-83

AIAA 6th Aerospace Sciences Meeting

NEW YORK, NEW YORK /JANUARY 22-24, 1968

AERODYNAMIC SHATTERING OF LIQUID DROPS*

A.A. Ranger and J.A. Nicholls
Department of Aerospace Engineering
The University of Michigan
Ann Arbor, Michigan

Abstract

New experimental and analytical results are reported for the problem of liquid drop shattering. Breakup is observed to occur as a result of the interaction between a drop and the convective flow field established by the passage of a shock wave over it. The purpose of this study, that supplements and extends earlier experimental and theoretical investigations, is to establish the influence of various parameters on the rate of disintegration and the time required for breakup to occur. This information is sought for a range of conditions considered pertinent to the development and propagation of detonation waves in a gas-liquid droplet medium. The conditions which have been studied involve shock waves in air moving over water drops $750-4400\,\mu$ in diameter at Mach numbers $M_S = 1.5-3.5$. The corresponding dynamic pressure range is 10-310 psia. Photographic, drop displacement, and breakup time information is presented. At the higher shock strengths, drop fragmentation begins in as little as 2 μsec and is complete in 135 μsec.

A model is formulated for the breakup phenomenon by considering that it results from a boundary layer stripping mechanism. The rate of disintegration is found by integrating over the thickness of the liquid boundary layer to determine the mass flux in the layer and by assuming that this flux leaves the drop surface at its equator. The experimental determination of the variation of drop shape and velocity with time is required to complete the calculation of disintegration rate and breakup time.

I. Introduction

The fragmentation of liquid drops resulting from their sudden exposure to a high velocity gas stream has many important applications in the fields of aerodynamics and propulsion. For example; the phenomenon of supersonic rain erosion, which is caused by the impingement of rain droplets at high relative speeds on exterior missile and aircraft surfaces, can be greatly alleviated through proper aerodynamic design. A reduction in the damage sustained from impacting drops is achieved by designing a body whose detached shock is sufficiently far removed to allow for drop shattering in the region separating the shock from the body surface. In regard to propulsion, the rate of mixing and combustion of liquid fuel droplets can be greatly enhanced by virtue of the fragmentation process. As a result of drop breakup higher burning rates, than are obtainable under low-velocity forced-convection conditions wherein no disintegration occurs, are obtainable. Specifically, this investigation arose in connection with a study of the development and propagation of a detonation wave in a gaseous (oxidizer)-liquid droplet (fuel) system, wherein the rate controlling mechanism is apparently the drop breakup time. This phenomenon is pertinent to liquid propellant rocket motor combustion instability.

A comprehensive survey of the literature on drop shattering was conducted by the authors[1]. Only those papers most pertinent to the present study will be mentioned here.

Engel[2], Hanson[3], Nicholson[4] and Wolfe[5], studied the shattering of liquid drops behind normal shock waves in a shock tube where the diameter, surface tension, density, and viscosity of the droplets and the Mach number of the shocks were varied. The results of these early experiments indicate that the major variables affecting the high speed breakup (Weber numbers much greater than 10) are the drop diameter and the dynamic pressure of the convective flow with the liquid properties being less important. Morrell[6] and Clark[7] studied the similar problem of liquid jet breakup induced by a transverse gas flow and their results can be compared with those of liquid drop shattering. More will be said of these earlier studies in the experimental results and discussion section.

All of the previous experiments were conducted at relatively low primary shock wave Mach numbers or low dynamic pressures and therefore do not cover the range of conditions characteristic of two-phase detonation. Consequently, the purpose of this work is to supplement and extend the earlier experimental and analytical investigations to find the rate of drop shattering, breakup times, drop displacement, and drop deformation for a range of conditions generated by two-phase detonations.

In the following sections the results of a shock tube investigation are presented followed by an

analytical treatment of boundary layer stripping from the drop. The experimental and theoretical results are then combined to examine the validity of the model.

II. Experimental Investigation

Experimental Apparatus

The experimental arrangement used in this study is shown schematically in Fig. 1. A stream of extremely stable, uniform size, equally spaced drops is obtained by vibrating a small jet of water at the Rayleigh instability frequency[8]. These drops fall vertically through the test section of a helium driven shock tube by means of an opening in the top and bottom. Since the test section is open to the atmosphere, the initial pressure in the driven section is $P_1 = 1$ atmosphere. A collimated beam of high intensity light is used to back-light the drops, and both image converter and rotating drum type cameras are employed to photograph the interaction phenomena. A more detailed description of the experimental equipment is given elsewhere[1].

The experimental procedure consists of obtaining a time history of the deformation, disintegration, and displacement of a drop by taking a series of individual shadow photographs at different time intervals after the shock wave intercepts the drop and by taking streak photographs.

A Beckman and Whitley Dynafax camera was employed to obtain the streak pictures. The individual photographs, which are .1 μsec exposures, were taken with a Beckman and Whitley Model 501A image converter camera. This camera is triggered by a thyratron circuit which is fired by a signal produced from a pressure switch located in the wall of the shock tube just upstream of the test section. A time delay unit is used to control the time that elapses between the moment that the shock passes this switch and the instant that the picture is taken. A measurement of the transit time between two pressure sensors was utilized to determine the shock speed. Extreme care was taken to insure that the testing time available was greater than the anticipated breakup time and that the drop separation distance was sufficient to rule out proximity effects.

Results and Discussion

The results discussed here are for experiments that cover the shock Mach number range of $M_s = 1.5$-3.5 in air with water drops having diameters in the range $D_0 = 750$-4400μ. Image converter and streak photographs of typical shock wave-water drop interactions are shown in Figs. 2-6. Drop deformation, displacement, and breakup time correlations are given in Figs. 7-13.
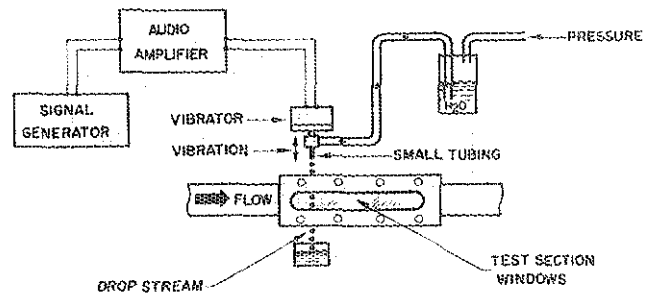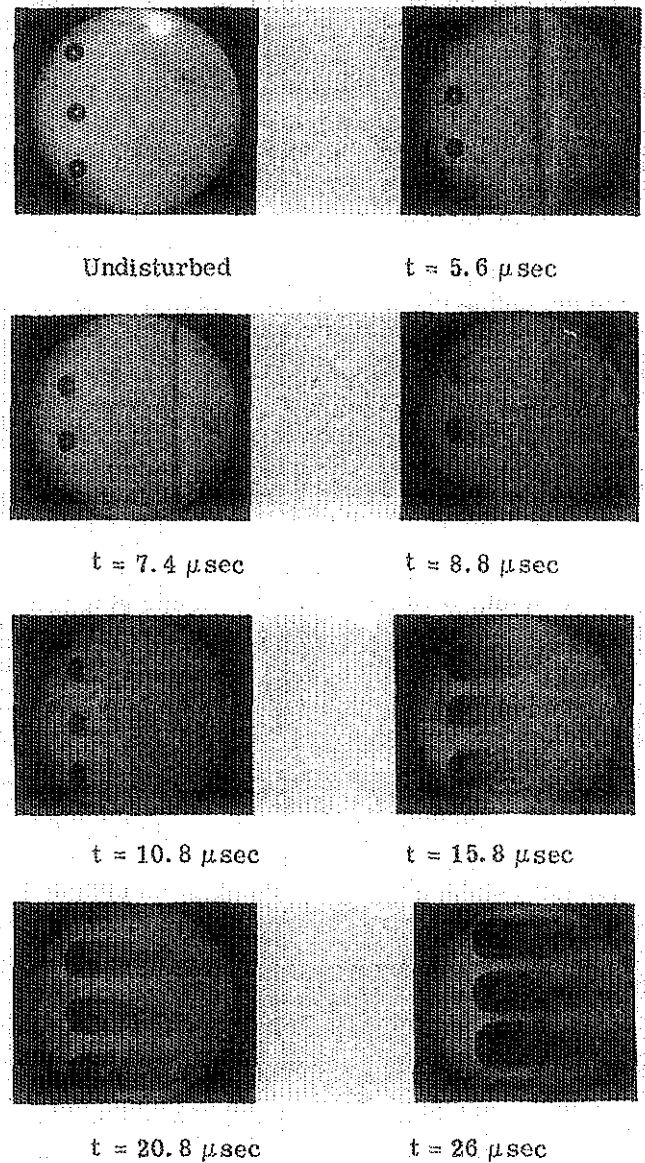

Fig. 1. Experimental Arrangement

Undisturbed	$t = 5.6 \mu$sec
$t = 7.4 \mu$sec	$t = 8.8 \mu$sec
$t = 10.8 \mu$sec	$t = 15.8 \mu$sec
$t = 20.8 \mu$sec	$t = 26 \mu$sec

Fig. 2. Shadow Photograph Sequence
$M_s = 2$, $D_0 = 750 \mu$

2

Figure 2 shows the sequence of events leading to the shattering of 750 μ drops by a $M_S = 2.0$ shock wave where initially the convective flow velocity relative to the motionless (in the stream direction) drop is approximately sonic and equal to 1415 ft/sec. The highlight which appears in the undisturbed drops is an image of the spark light source and it remains very bright and distinct until the growth of surface disturbances destroys the drop's ability to act as a focusing lens. In this sequence, the highlight disappears between 7.4 μsec and 8.8 μsec, and the planar incident shock wave that is visible in several of the pictures moves from left to right across the drops. The observed breakup can be temporally divided into two rather distinct stages. The first one, or dynamic stage, is the period during which the drops are flattened as a result of the external pressure distributions. Measurements from these and other such photographs establish for the first time that the deformed drops are planetary ellipsoids. The eccentricity of the elliptical profile changes with time. The second stage is characterized by a surface stripping process which is produced by the shearing action of the convective flow and which rapidly reduces the drops to clouds of micro-mist. At $t = 26$ μsec after the shock made initial contact with the drop, this latter stage is well developed.

When the incident shock Mach number is increased to $M_S = 2.7$, the deformation and disintegration of a drop no longer appear as distinct and separate stages of the breakup but occur almost simultaneously as seen in Fig. 3. For example, within only 4.4 μsec after the shock passage, a significant wake of micro-mist is formed behind the drop, and since the convective flow is supersonic with a Mach number = 1.28, a detached bow shock is also present in the photographs.
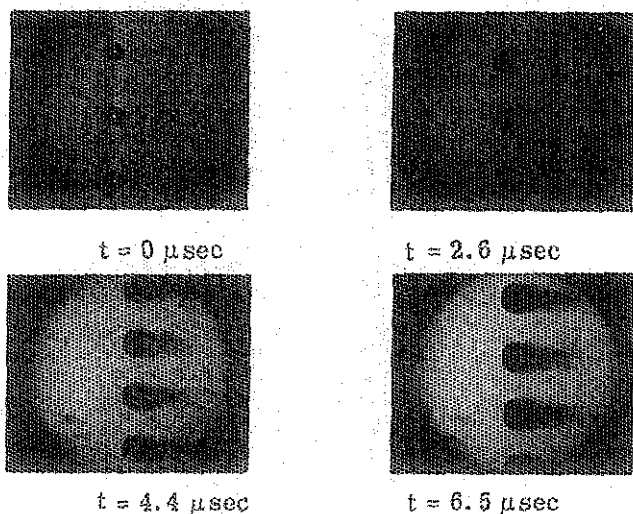
Figures 4 and 5 are presented to illustrate two important results. The vertical line passing through the center of the undisturbed drop in Fig. 4 is a fiducial marker on the test section window. First of all, it is observed that in only 14 μsec after a $M_S = 3.5$ air shock collides with a 2700 μ drop, a well defined wake is formed behind it. The interesting feature of this wake is that its shape is similar to that developed behind a hypersonic blunt body where the flow, as a result of strong lateral pressure gradients, also converges to form a narrow recompression neck region several body diameters downstream of the rear stagnation point. The very fact that the liquid material being continuously stripped off from the surface of the drop is able to follow the streamline pattern of the wake indicates that the drop is reduced to a fine micro-mist. If the drop were being eroded away in rather massive
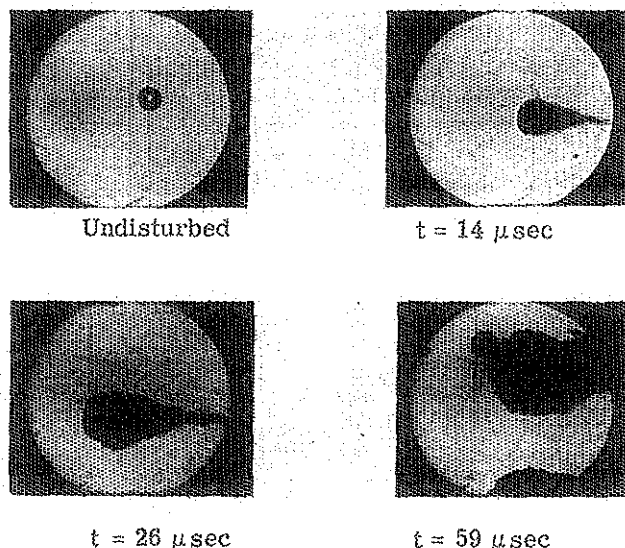

Undisturbed   t = 14 μsec

t = 26 μsec   t = 59 μsec

Fig. 4. Shadow Photograph Sequence
$M_S = 3.5$, $D_O = 2700 \mu$

t = 0 μsec   t = 2.6 μsec

t = 4.4 μsec   t = 6.5 μsec

Fig. 3. Shadow Photograph Sequence
$M_S = 2.7$, $D_O = 750 \mu$

Undisturbed   t = 38.8 μsec

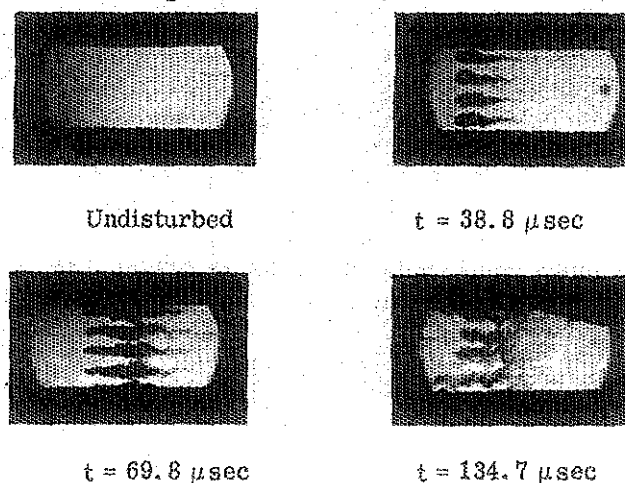t = 69.8 μsec   t = 134.7 μsec

Fig. 5. Shadow Photograph Sequence
$M_S = 3.3$, $D_O = 1090 \mu$

3

pieces, which by reason of their inertia were unable to follow the streamlines, the shape of the wake would be entirely different from the one visible in the photographs. Secondly, the pictures of the 1090 μ drops, taken at a smaller magnification to include the entire wake, along with other data reveal that the breakup is a continuous process of disintegration that begins shortly after the initial contact between a shock and a drop and proceeds until the drop is completely transformed into a cloud of mist. For purposes of this study, the breakup is defined as complete when the wake has the diffuse appearance evident in the photograph taken at t = 134.7 μsec after shock passage.

The effect of shock Mach number on the rate of breakup and on the acceleration can be vividly seen in Fig. 6. The two streak photographs show the continuous displacement of an 1100 μ drop as a function of time when the incident shock strength is (a) M_s = 1.6 and (b) 2.5. The displacement (x) and time (t) axes are scaled such that the distance between adjacent horizontal fiducial lines is one inch and this unit of length along the time axis is equivalent to 86 μsec. Disintegration is seen to begin within several microseconds after the Mach 2.5 shock intercepts the drop whereas approximately 50 μsec elapse before stripping is apparent at the lower Mach number. It is interesting to
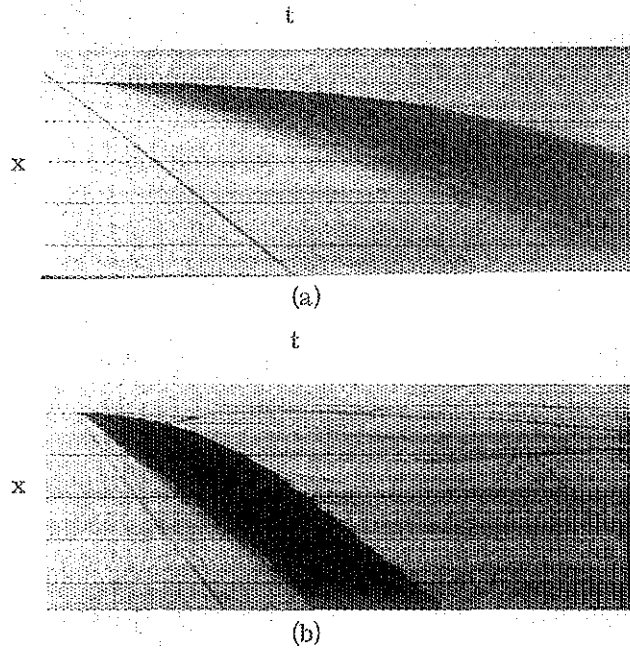

(a)

(b)

Fig. 6. Streak Photographs
(a) M_s = 1.6, (b) M_s = 2.5, D_o = 1100 μ.

note that in both cases the material which is initially removed from the drop surface is accelerated almost instantaneously to the particle velocity behind the wave front thus giving some indication of the small size of these particles. Since

the convective flow is supersonic relative to the drop, one also notes the presence of a stand-off bow shock and several wake shocks when M_s = 2.5.

The deformation of a drop as defined by the ratio of maximum diameter to the original diameter is plotted in Fig. 7 as a function of time. Some experimental results of Engel[2] are included in this figure. One observes that the time required to reach an equivalent state of deformation decreases and the maximum diameter attained increases as the incident shock Mach number goes from M_s = 1.3-3.5. For example, when M_s = 1.3, the time required for a 2700 μ drop to reach its maximum deformation of 3.2 D_o is 320 μsec whereas at M_s = 3.5 it only takes 55 μsec to attain a deformation ratio of 3.8.

Typical displacement data obtained from the experiments are plotted in Fig. 8 and compared with parabolic relations (constant acceleration) between distance and time. Good agreement is apparent between the parabolic curves and the data during the initial phases of the breakup; however it degenerates in the latter phases, thus indicating that while initially the drop acceleration is reasonably constant, it does not remain so during the advanced portion of the breakup. Physically this indicates that approximately midway through the breakup period the mass of a drop is decreasing at a rate faster than the drag forces are diminishing and the net effect is an increase in the drop acceleration.
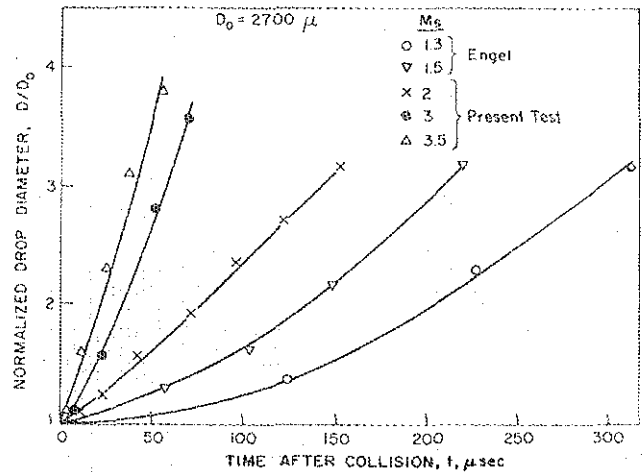

Fig. 7. Drop Deformation

In spite of the last qualification it is interesting to consider the drop as a spherical particle of constant mass and then write the momentum equation, i.e.

$$C_D \frac{1}{2} \rho_g U_r^2 S = Ma$$

4

or,

$$a = \frac{3}{4} \frac{C_D}{D} \frac{\rho_g}{\rho_\ell} U_r^2 \quad . \tag{1}$$

Now, assuming constant acceleration

$$x = \frac{1}{2} a t^2 = \frac{3}{8} \frac{C_D}{D} \frac{\rho_g}{\rho_\ell} U_r^2 t^2 \quad ,$$

or in dimensionless terms with C_D, D, and U_r evaluated at $t = 0$ (ρ_g and ρ_ℓ are invariant with t), we get

$$\overline{X} = \frac{3}{8} C_{D_0} \overline{T}^2 \quad . \tag{2}$$

In view of Eq. (2), the displacement data for a variety of drop sizes and shock strengths (including some data from Engel[2] and Nicholson[4]) are plotted against the non-dimensional variables with the result shown in Fig. 9. The family of parabolas in Fig. 8 collapse into the single parabola $\overline{X} = 1.1 \overline{T}^2$ except for the data of Nicholson which better fits $\overline{X} = 0.714 \overline{T}^2$. The constant of 1.1 implies a $C_{D_0} \cong 3$.
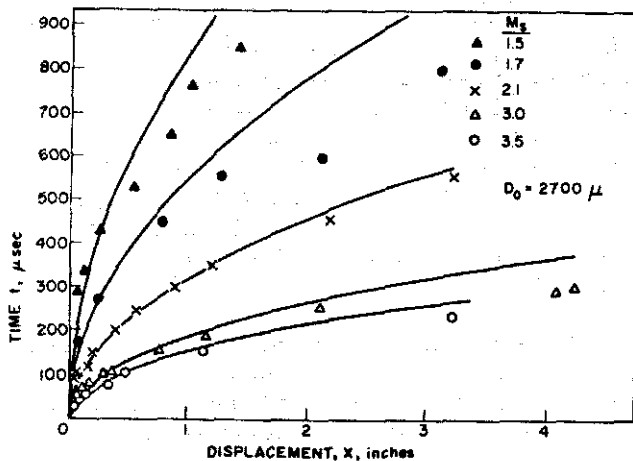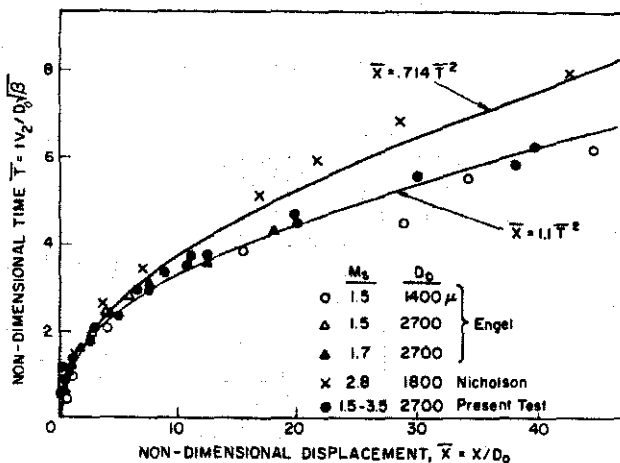

Fig. 8. Drop Displacement

Fig. 9. Dimensionless Displacement

The effect of incident shock strength on the time required to breakup a drop of a given diameter is shown in Fig. 10. For example, less than 100 μsec is required to completely disintegrate a 900 μ drop at $M_s = 3.5$ whereas 360 μsec is needed when $M_s = 1.5$. The apparent discrepancy between Nicholson's data and these results is explained by the fact that Nicholson used various reduced initial pressures (P_1) for purposes of altitude simulation studies. Since a reduction in the initial driven section pressure has the effect of producing a lower dynamic pressure for a given Mach number, the breakup times he observed were larger than those produced in either this or Engel's study. If the dimensionless breakup time, $\overline{T}_b$, is evaluated from this data it is found that, approximately, $\overline{T}_b = 5$. However, there is a M_s effect in that $\overline{T}_b$ varies from about 5-6 as M_s goes from 1.5-3.5. Using the value of 5, then $\overline{X}_b \cong 28$; that is to say, the drop displacement distance for breakup is about 28 diameters. A comparison between dimensionless breakup times can be made by rewriting Clark's[7] expression in terms of $\overline{T}$ to get $\overline{T}_b = \sqrt{\epsilon_b}$. Using a value of $\epsilon_b = 15$, corresponding to complete breakup, one finds a $\overline{T}_b \simeq 4$ which is in reasonable agreement with the value evaluated from the present study.
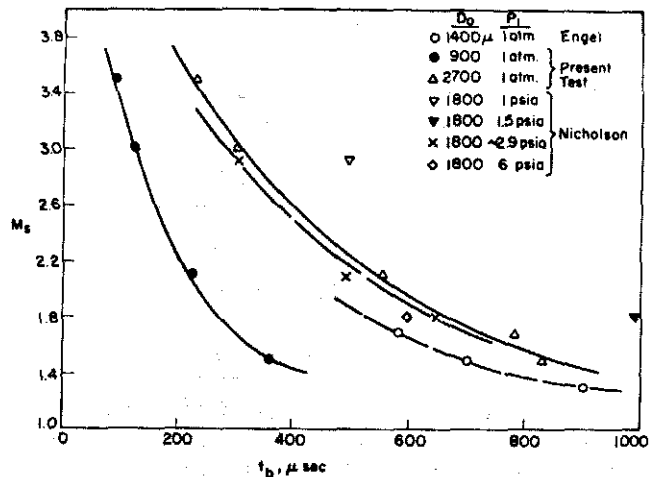

Fig. 10. Effect of Mach Number

The effect of the dynamic pressure on the time required for breakup is shown in Fig. 11 where it is apparent that low dynamic pressures correspond to extremely long breakup times and, conversely, high pressures indicate rapid breakup. Thus the importance of the dynamic pressure as a variable in the shattering process is firmly established. Of course, the importance of this is also indicated by the $\overline{X}$, $\overline{T}$ correlation and the definition of $\overline{T}$.

If the drop deformation data are plotted against the non-dimensional time, $\overline{T}$, a distribution is obtained such as that shown in Fig. 12. Although some scatter is evident it is reasonable to assume

5

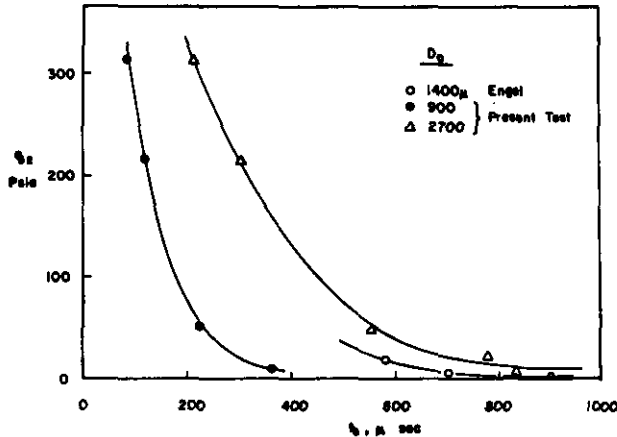that a two part linear approximation to the distribution is acceptable.
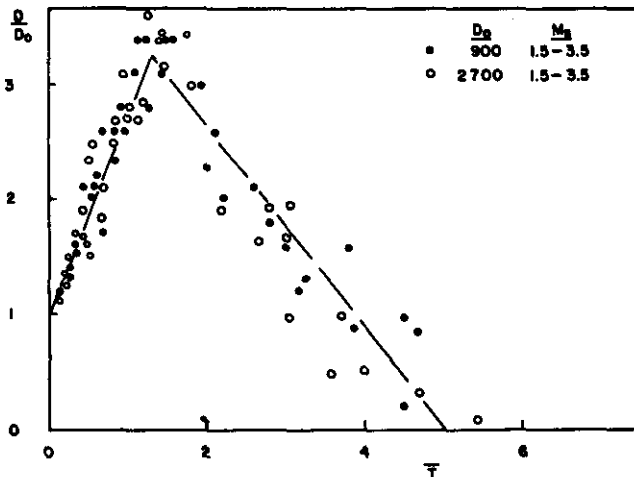

Fig. 11. Effect of Dynamic Pressure

Fig. 12. Deformation Distribution

Using for the displacement the relation $\overline{X} = 1.1\,\overline{T}^2$, the relative velocity between an accelerating drop and the convective flow behind the shock front can be computed. These computations are plotted versus $\overline{T}$ in Fig. 13 with the shock Mach number as a parameter. The results indicate that at breakup, when $\overline{T} \simeq 5$, the relative velocity has diminished to approximately 50% of its initial value when $M_S = 1.3$ whereas at $M_S = 3.5$ it is only 20%.

III. Boundary Layer Stripping Analysis

It is apparent from the photographs that the collision between the incident shock and the drop has little if any effect on the shattering phenomenon, and thus breakup occurs as a result of the interaction between a drop and the convective flow field established by the shock. Therefore in formulating a model for shock wave-drop interaction, one can neglect the shock altogether and treat the problem simply as a droplet in a high speed flow.
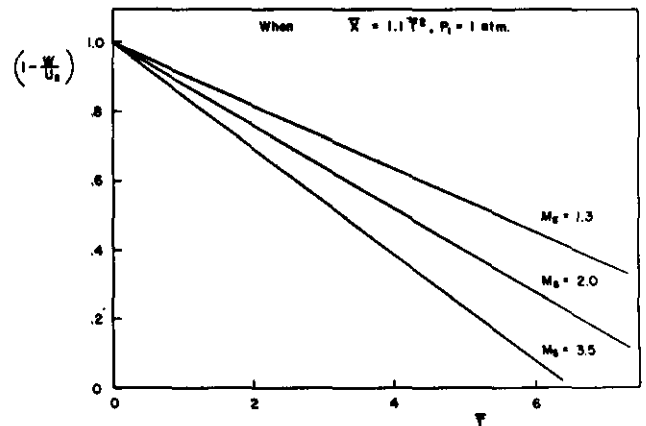

Fig. 13. Relative Velocity Distribution

The shearing action exerted by the high speed gas stream on the drop periphery causes the formation of a boundary layer in the surface of the liquid. Calculations indicate that this layer can be established very rapidly after a drop is intercepted by a shock, and the photographs show it being stripped away from the equator.

On the basis of these experimental observations, a model is formulated for the breakup phenomenon by considering that disintegration results from a boundary layer stripping mechanism. The rate of disintegration is found by integrating over the thickness of the liquid boundary layer to determine the mass flux in the layer and by assuming that this flux leaves the surface of the drop at its equator. In order to evaluate the mass flux, we utilize a form of analysis attributable to G. I. Taylor[9].

Consider therefore the sudden exposure of a liquid drop to a high speed gas stream. Boundary layers will form in each as shown in Fig. 14 where x is the curvilinear coordinate along the interface separating the two fluids and y is the coordinate perpendicular to it. An approximate solution to the two-boundary-layer problem can be obtained
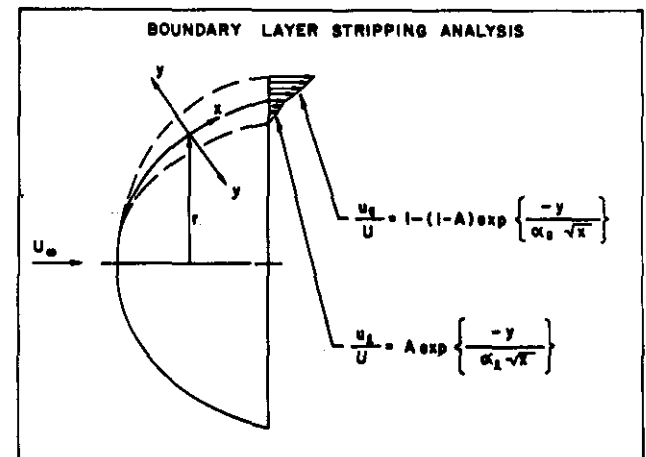

Fig. 14. Boundary Layer Model

6

by assuming arbitrary simple velocity distributions containing a few parameters and then using the momentum integral relations to determine those parameters.

If we assume that the flow is steady and incompressible, then the boundary layer momentum integral equations are for the gas

$$\frac{\partial}{\partial x}\int_0^\infty u_g (U - u_g) \, dy + \frac{dU}{dx}\int_0^\infty (U - u_g) \, dy$$

$$+ \frac{1}{r}\frac{dr}{dx}\int_0^\infty u_g (U - u_g) \, dy = \nu_g \left(\frac{\partial u_g}{\partial y}\right)_{y=0}, \quad (3)$$

and for the liquid

$$\frac{\partial}{\partial x}\int_0^\infty u_\ell^2 \, dy + \frac{1}{r}\frac{dr}{dx}\int_0^\infty u_\ell^2 \, dy = - \nu_\ell \left(\frac{\partial u_\ell}{\partial y}\right)_{y=0}$$

$$- \frac{1}{\rho_\ell}\frac{dp}{dx}\delta_\ell, \quad (4)$$

where the pressure gradient in the liquid layer is given by $dp/dx = - \rho_g U (dU/dx)$. Equating the shear stress in the gas layer to that in the liquid layer at the interface yields a third equation

$$- \rho_\ell \nu_\ell \left(\frac{\partial u_\ell}{\partial y}\right)_{y=0} = \rho_g \nu_g \left(\frac{\partial u_g}{\partial y}\right)_{y=0}. \quad (5)$$

We assume that the velocity distributions in the liquid and gas are given respectively by the simplified but convenient expressions from Taylor[9]; i.e.

$$\frac{u_\ell}{U} = A \exp\left\{\frac{-y}{\alpha_\ell \sqrt{x}}\right\},$$

$$\frac{u_g}{U} = 1 - (1 - A) \exp\left\{\frac{-y}{\alpha_g \sqrt{x}}\right\}, \quad (6)$$

where A is the dimensionless velocity at the interface. The drop shape, which is actually ellipsoidal, can be approximated by a sphere for the simplified analysis here and hence

$$U = \frac{3}{2} U_\infty \sin (x/R), \quad (7)$$

$$r = R \sin (x/R), \quad (8)$$

then, applying Eq. (6-8) to (3-5), we obtain the three equations

$$\frac{3}{8} U_\infty (1 + A) \alpha_g = \frac{\nu_\ell}{\alpha_g}, \quad (9)$$

$$\frac{3}{8} U_\infty A \alpha_\ell = \frac{\nu_\ell}{\alpha_\ell} \quad (10)$$

$$\rho_\ell \nu_\ell \frac{A}{\alpha_\ell} = \rho_g \nu_g \frac{(1-A)}{\alpha_g} \quad (11)$$

which are valid at the equator of a sphere; i.e. at $x/R = \pi/2$. From Eq. (10) we have

$$\alpha_\ell = \left[\frac{8}{3}\frac{\alpha_\ell}{A U_\infty}\right]^{1/2}, \quad (12)$$

and from Eq. (11)

$$\alpha_g = \alpha_\ell \frac{\rho_g}{\rho_\ell}\frac{\nu_g}{\nu_\ell}\frac{(1-A)}{A}, \quad (13)$$

which when substituted into Eq. (9) gives

$$\left[1 - \left(\frac{\rho_\ell}{\rho_g}\right)^2\left(\frac{\nu_\ell}{\nu_g}\right)\right]A^3 - A^2 - A + 1 = 0 \quad (14)$$

Since A must be small compared to unity, one observes from Eq. (14) that A^3 must be of the order $(\rho_g/\rho_\ell)^2 (\nu_g/\nu_\ell)$. Therefore we put

$$A = \left(\frac{\rho_g}{\rho_\ell}\right)^{2/3}\left(\frac{\nu_g}{\nu_\ell}\right)^{1/3} \quad (15)$$

The mass of fluid in the circumferential liquid layer being swept along by the gas stream at a distance $x = \pi D/4$ from the stagnation point is

$$\frac{dm}{dt} = \pi D \rho_\ell \int_0^\infty u_\ell \, dy = \frac{3}{4}(\pi D)^{3/2}\rho_\ell A \alpha_\ell U_\infty, \quad (16)$$

or substituting for A and α_ℓ, Eq. (16) becomes

$$\frac{dm}{dt} = \sqrt{\frac{3}{2}\pi^3}\left(\frac{\rho_g}{\rho_\ell}\right)^{1/3}\left(\frac{\nu_g}{\nu_\ell}\right)^{1/6}\left(\rho_\ell \nu_\ell^{1/2} U_2^{1/2} D_0^{3/2}\right)$$

$$\times \left(\frac{D}{D_0}\right)^{3/2}\left(1 - \frac{w}{U_2}\right)^{1/2}, \quad (17)$$

where U_∞ has been replaced by the relative velocity. Therefore, the total mass stripped away during a period equal to $\overline{T}$ is found by integrating Eq. (17) with respect to time to obtain

$$m = \sqrt{\frac{3}{2}\pi^3}\left(\frac{\rho_g}{\rho_\ell}\right)^{-1/3}\left(\frac{\mu_g}{\mu_\ell}\right)^{1/6}\left(\rho_\ell \nu_\ell^{1/2} U_2^{-1/2} D_0^{5/2}\right)$$

$$\times \int_0^{\overline{T}}\left(\frac{D}{D_0}\right)^{3/2}\left(1 - \frac{w}{U_2}\right)^{1/2} d\overline{T}. \quad (18)$$

In the absence of an analytical solution for the detailed dynamics of the drop, the integrand cannot be evaluated. Accordingly, one must resort to the experimental data. The validity of the boundary layer stripping model is supported by the fact that when one sets $\bar{T}_b = 5$ and uses the distributions for (D/D_o) and $(1 - w/U_2)$ shown in Figs. 12 and 13 to evaluate Eq. (16), the calculated total mass removed is quite close to the original mass of the drop. The agreement is within about 10% and appears to hold for both incompressible and compressible flow conditions even though the analysis is strictly incompressible.

IV. Conclusions

The impact by a strong shock wave is an insignificant element in producing the shattering of a liquid drop. The main function of the shock is to produce the high speed convective flow which is responsible for the disintegration. A drop which is originally spherical is deformed into a planetary ellipsoid with its major axis perpendicular to the direction of flow. The shearing action exerted by the high speed flow causes a boundary layer to be formed in the surface of the liquid and the stripping away of this layer accounts for the breakup. These studies further support the fact that the breakup time is proportional to the drop diameter, inversely proportional to the velocity, and proportional to the square root of the liquid to gas density ratio.

References

1. Dabora, E.K., Ragland, K.W., and Ranger, A.A., "Two Phase Detonations and Drop Shattering Studies," University of Michigan, Second Annual Progress Report 06324-2-T, April 1966.

2. Engel, O.G., "Fragmentation of Waterdrops in the Zone Behind an Air Shock," J. of Res. Nat'l. Bur. Standards, Vol. 60, No. 3, March 1958.

3. Hanson, A.R., Domich, E.G., and Adams, H.S., "An Experimental Investigation of Impact and Shock Wave Break-up of Liquid Drops," Res. Rept. 125, Rosemount Aero. Lab., Minneapolis, Minn., January 1956.

4. Nicholson, J.E. and Hill, A.F., "Rain Erosion on Spike Protected Supersonic Radomes," Mithras, Inc., Cambridge, Mass., MC-61-6-R3, April 1965.

5. Wolfe, H. and Andersen, W., "Aerodynamic Break-up of Liquid Drops," American Physical Society Paper SP70, April 1965.

6. Morrell, G. and Povinelli, F.P., "Break-up of Various Liquid Jets by Shock Waves and Applications to Resonant Combustion," NASA TN D-2423.

7. Clark, B.J., "Breakup of a Liquid Jet in a Transverse Flow of Gas," NASA TN D-2424.

8. Dabora, E.K., "Production of Monodisperse Sprays," Rev. Sci. Instr., 38, 502-506 (April 1967).

9. Taylor, G.I., "The Shape and Acceleration of a Drop in a High-Speed Air Stream," Collected works of G.I. Taylor.

Nomenclature

A	dimensionless interface velocity
a	drop acceleration (dw/dt)
C_D	drag coefficient
D	drop diameter
M, m	droplet mass
M_s	shock Mach number
P, p	static pressure
q	dynamic pressure
R	drop radius
S	drop frontal area $(\pi D^2/4)$
t	time after collision
$\bar{T}$	dimensionless time $\left[t\,(\dot{U}_2/D_o)\,\sqrt{\beta} \right]$
U	fluid velocity
u	boundary layer velocity
w	drop velocity
x	drop displacement
$\bar{X}$	dimensionless displacement (x/D_o)
α	boundary layer shape factor
β	gas-to-liquid density ratio (ρ_g/ρ_ℓ)
μ	fluid viscosity (also implies micro and micron)
ν	kinematic viscosity
ρ	fluid density

Subscripts

1	refers to initial conditions
2	refers to shocked conditions
b	refers to breakup
g	refers to gas
ℓ	refers to liquid
o	refers to $t = 0$
r	relative velocity
∞	free stream velocity